Scattering Analysis for the Modeling of THz Communication Systems

Radoslaw Piesiewicz, *Student Member, IEEE*, Christian Jansen, *Student Member, IEEE*, Daniel Mittleman, Thomas Kleine-Ostmann, Martin Koch, and Thomas Kürner, *Senior Member, IEEE*

***Abstract*—Modeling propagation channels for future pico-cellular indoor THz communication systems requires the knowledge of the reflective properties of building materials. The reflectivity of smooth, optically thick materials can be modeled with Fresnel equations. In case of materials with a rough surface, diffuse scattering reduces the power reflected in the specular direction. Kirchhoff scattering theory can be employed to derive modified Fresnel equations which account for these losses by introducing a Rayleigh roughness factor calculated from the measured surface height distribution of the sample under observation. Using the resulting, analytically derived reflection coefficient based on material parameter and surface measurements in propagation models enables the simulation of arbitrary configurations. We present a set of calculated and measured reflection coefficients for a selection of common indoor building materials which are in good agreement, thus verifying our modeling approach. Furthermore, we illustrate by ray-tracing simulations the effect of wall and ceiling roughness on propagation in future indoor scenarios. Both, absolute power levels and propagation patterns are shown to be strongly influenced by scattering. In some cases, reflected transmissions with longer propagation paths can be more efficient than the shorter ones in terms of incurred losses.**

***Index Terms*—Kirchhoff approximation, ray-tracing, rough surface scattering, THz channel modeling, THz communication.**

I. Introduction

THE increasing demand for higher data rates in wireless communications is shifting attention towards frequencies above 100 GHz [1], [2]. Future indoor wireless communication systems will have to support data rates of tens of Gbps [3] and will need very large bandwidths. They might be accommodated in the THz range and could potentially work with directed transmissions supported by omni-directional dielectric mirrors [4], [5]. The first two atmospheric frequency windows, which might be used for such systems in the future are centered at 300 and 350 GHz, respectively.

Before the introduction of such systems, the THz propagation channel must be thoroughly investigated. We use site-specific modeling, implemented with ray-tracing to calculate the spatial channel properties [4]. Its reliability depends on the accuracy of the estimated signal propagation in the modeled environment. In case of future THz communication systems which will rely on directed high gain antennas, accurate prediction of reflection losses in the specular direction will be crucial for determining the channel behavior. Reflection losses of building materials in the THz range can be measured for chosen angles of incidence [6] or modeled for arbitrary ones. An efficient method to model reflective properties of building materials, based on Fresnel equations and measured material parameters was proposed in [7]. However, this technique is limited to smooth materials only, as scattering losses are not taken into account. Scattering properties of building materials at THz frequencies have not yet been studied for the modeling of propagation for communication purposes. Yet, the reduction of the reflected power in the specular direction due to diffuse scattering cannot be neglected when modeling propagation effects with high gain antennas in realistic environments with a substantial amount of rough surface materials. Also, robust scattering models are needed that can be implemented in ray-tracing algorithms to enhance the propagation modeling.

In general, the problem of rough surface scattering can be solved with numerical simulation approaches that are based on integral or differential equation methods to solve the underlying Maxwell boundary value problem [8], [9]. However, numerical approaches are rather complex and usually time-intensive. Instead, under certain conditions analytical approximations can be used. Such algorithms are very robust, give physical insight into the problem and can be easily implemented in ray-tracing. Here, we extend the method which we presented in [7] and which accounts for the reflectivity of smooth materials above 100 GHz, in order to model reflective properties of rough materials in the specular direction. The extension utilizes the Kirchhoff theory of scattering from rough surfaces [10], which is implemented into the existing model by multiplication of the reflection coefficient derived from the Fresnel equations with a Rayleigh roughness factor. This factor can be calculated from measured surface roughness data of the investigated material. The extended model is verified by the measurement of reflection data for common

Manuscript received October 27, 2006; revised January 12, 2007.

R. Piesiewicz and T. Kürner are with the Institute for Communications Technology, Technical University of Braunschweig, Braunschweig 38106, Germany and also with the Terahertz Communications Lab, Braunschweig 38106, Germany (e-mail: piesiewicz@ifn.ing.tu-bs.de; t.kuerner@tu-bs.de).

C. Jansen is with the Institute for High Frequency Technology, Technical University of Braunschweig, Braunschweig 38106, Germany (e-mail: c.jansen@gmx.de).

D. Mittleman is with the Electrical Engineering Department, Rice University, Houston, TX 77005 USA (e-mail: daniel@rice.edu).

T. Kleine-Ostmann is with the Physikalisch-Technische Bundesanstalt, 38116 Braunschweig, Germany and also with the Terahertz Communications Lab, Braunschweig 38106, Germany (e-mail: Thomas.Kleine-Ostmann@ptb.de).

M. Koch is with the Institute for High Frequency Technology, Technical University of Braunschweig, Braunschweig 38106, Germany and also with the Terahertz Communications Lab, Braunschweig 38106, Germany (e-mail: m.koch@tu-bs.de).

Color versions of one or more of the figures in this paper are available online at http://ieeexplore.ieee.org.

Digital Object Identifier 10.1109/TAP.2007.908559

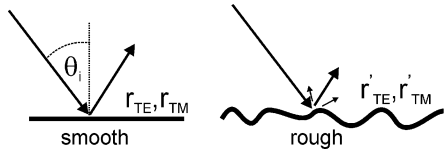

Fig. 1. Reflection from a smooth (left) and from a rough (right) surface.

building materials with rough surfaces in the frequency range from 0.1 to 1 THz.

The paper is structured as follows: in Section II the modified Fresnel equations that model scattering in the specular direction are introduced and the surface roughness measurements as well as the calculation of the roughness parameters are shown for common building materials. Section III presents reflection measurements and compares them with simulations based on simple and modified Fresnel equations as introduced in Section II. Also, in this section ray-tracing signal coverage calculations in a simple indoor scenario with smooth materials are compared to simulations in a corresponding scenario with rough materials to underline the importance of proper modeling of the propagation environment. Concluding remarks wrap up this paper in Section IV.

II. Rough Surface Scattering

A. Modified Fresnel Equations

The reflection of a plane wave from a smooth and from a rough surface is schematically shown in Fig. 1.

In order to account for scattering losses in the specular direction, the Fresnel reflection coefficients must be multiplied by the Rayleigh roughness factor [10]

$$\rho = e^{-\frac{g}{2}}$$

with

$$\mathrm{g} = \left(\frac{4\pi \cdot \sigma \cdot \cos\Theta_\mathrm{i}}{\lambda}\right)^2. \tag{1}$$

Here, Θ_i is the angle of incidence and reflection, σ the standard deviation of the surface roughness and λ the free space wavelength of the incident wave. The modified reflection coefficients $\mathrm{r}'_{\mathrm{TE}}$ and $\mathrm{r}'_{\mathrm{TM}}$ that model the reduction of the signal power in the specular direction are then

$$r'_{\mathrm{TE}} = \rho \cdot r_{\mathrm{TE}}$$

and

$$r'_{\mathrm{TM}} = \rho \cdot \mathrm{r}_{\mathrm{TM}} \tag{2}$$

where r_{TE} and r_{TM} are the Fresnel reflection coefficients for a smooth surface in the case of TE or TM polarized waves, respectively, which can be efficiently and reliably calculated in the THz range from the frequency dependent index of refraction n and absorption coefficient α [7] by

$$r_{\mathrm{TE}} = \frac{Z\cos\Theta_i - Z_0\cos\Theta_t}{Z\cos\Theta_i + Z_0\cos\Theta_t}$$

and

$$r_{\mathrm{TM}} = \frac{Z\cos\Theta_t - Z_0\cos\Theta_i}{Z\cos\Theta_t + Z_0\cos\Theta_i}. \tag{3}$$

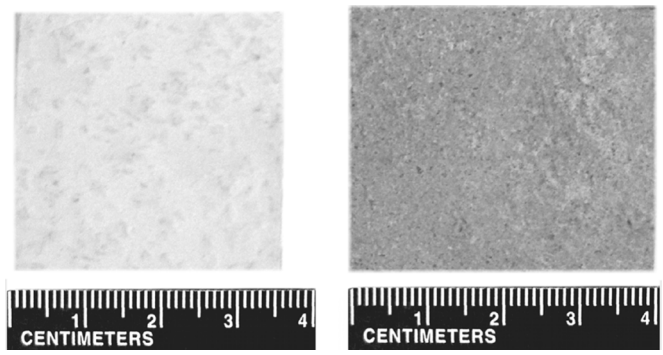

Fig. 2. Investigated materials: ingrain wallpaper (left) and concrete plaster (right).

Here, $\Theta_t = \arcsin(\sin(\Theta_i)\cdot Z/Z_0)$ is the angle of refraction, $Z_0 = 377\ \Omega$ the free space wave impedance and Z the wave impedance of the reflecting material, which is calculated using the expression

$$Z = \sqrt{\frac{\mu_0}{\varepsilon_0\left(n^2 - \left(\frac{\alpha c}{4\pi f}\right)^2 - j\frac{2n\alpha c}{4\pi f}\right)}} \tag{4}$$

where μ_0 and ε_0 are free space permeability and permittivity, c the velocity and f the frequency of the incident wave.

The Kirchhoff solution to the scattering problem assumes that there is no multiple scattering, no shadowing and that the surface is locally smooth, i.e., there are no sharp edges or corners. Furthermore, (2) will only deliver accurate results if the surface height distribution is Gaussian and the correlation length of the surface (see below) exceeds the wavelength [11].

B. Surface Roughness Characterization

Here, we investigate three planar samples of two common building materials as shown in Fig. 2.

One sample consists of ingrain wallpaper (Raufaser) glued on paperboard while the other two samples are pieces of concrete plaster with different roughness. The average thickness is 6.5 mm for the ingrain wallpaper on paperboard and 8.6 mm for the plaster samples. These materials are very common in indoor environments and are hence representative examples for propagation modeling.

The surface roughness of the samples is measured using commercially available equipment for optical 3D micro- and nanometrology [12]. With a 5x objective, lateral and vertical resolutions of 25 μm and 5 μm are achieved, respectively. The surface height distribution $h(x,y)$ of the samples is obtained by processing the measured surface roughness data which has been offset to a zero mean value. Histograms of the measured surface height distribution for the examined samples are shown in Fig. 3.

The surface roughness of the samples is approximated by a Gaussian distribution. The calculated standard deviation σ of the surface height of the samples is shown in Table I.

As σ is part of the exponent in the Rayleigh factor it has a strong influence on the modified reflection coefficients presented in (2).

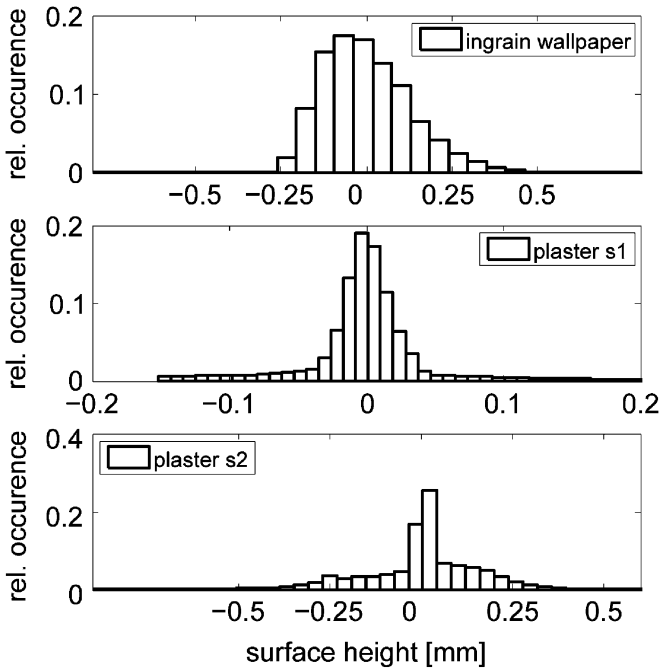

Fig. 3. Histograms of measured surface height offset to zero mean of ingrain wallpaper (top), plaster sample 1 (middle) and plaster sample 2 (bottom).

TABLE I
CALCULATED STANDARD DEVIATIONS FOR THE EXAMINED SAMPLES

sample	wallpaper	plaster s1	plaster s2
σ [mm]	0.13	0.05	0.15

It is clear from (1), that the roughness factor of a material depends on frequency and angle of incidence. Physically, this dependence can be explained with phase effects of the Kirchhoff solution that trace back to the relationship between surface roughness and wavelength, expressed with the ratio σ/λ as well as to the cosine function of the angle of incidence. A good measure of roughness is given by the parameter g. If its value is much smaller than 1 then the surface roughness is small and the power in the specular direction is only slightly reduced. For values of g near 1 the surface is moderately rough and the specular reflectance is diminished, but still considerably stronger than in non-specular directions. The values of g greater than 1 stand for very rough surfaces where diffuse scattering dominates the reflection behavior. Furthermore, due to the cosine function in the g factor formula, the effective surface roughness seen by an incoming wave is smaller towards higher angles of incidence. For the samples at hand the parameter g is shown in Fig. 4 for the frequency range between 100 GHz and 1 THz for two angles of incidence: 25° and 60°.

The values of g for the ingrain wall paper and plaster sample 2 are much bigger than the values of g for plaster sample 1. For all angles of incidence and frequencies above 300 GHz the absolute values of g for ingrain wallpaper and plaster sample 2 are greater than 1, so that a significant reduction of the reflection coefficient is expected. The g factor of plaster sample 1 has a value greater than 1 only for smaller angles of incidence or

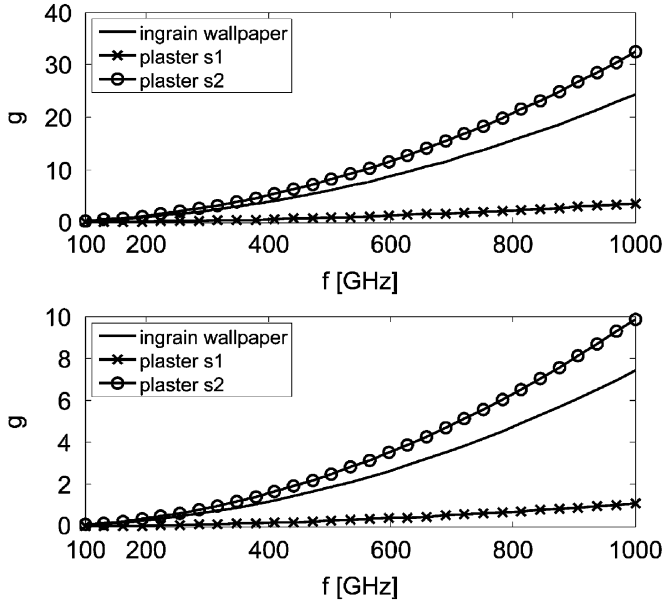

Fig. 4. Calculated parameter g for the three samples for angles of incidence of 25° (top) and 60° (bottom).

higher frequencies. Hence, a significant reduction of the reflection coefficient of plaster sample 1 is expected in a more limited range of angles of incidence and frequencies than in the case of the other two samples.

In order to further verify the validity of the employed Kirchhoff approach we calculate the correlation length for the samples. This figure of merit provides information about the correlation of the height of neighboring points on the surface, i.e., whether the irregularities are densely packed or not. Physically, this criterion verifies the assumption of local surface smoothness and gives a quantitative statement about the wavelengths at which phase effects are dominating over amplitude effects. If two different points on the surface are $p_1 = (x_1, y_1)$ and $p_2 = (x_2, y_2)$ then the corresponding heights are $h_1 = h(p_1)$ and $h_2 = h(p_2)$. The correlation function $C(\tau)$ for the points on the surface is then defined as [10]

$$C(\tau) = \frac{E(h_1 h_2)}{E\left(h_1^2\right)} \tag{5}$$

where τ is the distance between the points p_1 and p_2 and E is the expectation operator. The correlation length T is then defined as the distance τ for which the correlation function $C(\tau)$ drops to e^{-1}. The calculated correlation functions $C(\tau)$ of the samples are shown in Fig. 5.

Corresponding correlation lengths T are listed in Table II, together with the frequencies f_T for which the free-space wavelength is equal to the correlation length T.

For frequencies greater than f_T, the correlation lengths are greater than the wavelength of the incident wave. For all investigated samples the constraint that the correlation length must be greater than the wavelength [11] is met already for frequencies well below 300 GHz so that accurate results can be expected.

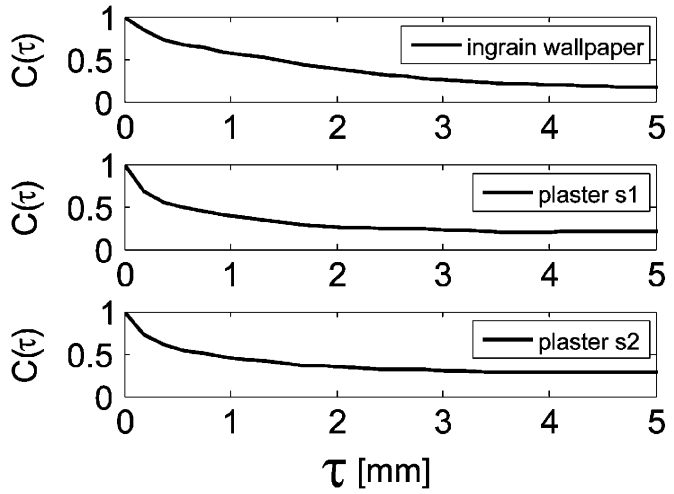

Fig. 5. Calculated correlation functions of the samples: ingrain wallpaper (top), plaster sample 1 (middle), and plaster sample 2 (bottom).

TABLE II
CALCULATED CORRELATION LENGTHS T FOR THE EXAMINED SAMPLES AND CORRESPONDING FREQUENCIES WHERE THE WAVELENGTH IS EQUAL TO THE CORRELATION LENGTH

sample	wallpaper	plaster s1	plaster s2
T [mm]	2.3	1.3	1.7
f_T [GHz]	130	230	176

III. THz MEASUREMENTS AND REFLECTION SIMULATIONS

A. Transmission and Reflection Measurements

We measure the absorption coefficient and the refractive index of the investigated samples with THz time-domain spectroscopy in transmission geometry as in [7]. Then, we calculate the reflection coefficients in the specular direction from the modified Fresnel equations. In order to verify our method we compare our calculations with THz time-domain measurements performed in reflection geometry. Both, transmission and reflection measurements are performed using a commercially available THz time-domain spectrometer with fiber-coupled transmitter and receiver [13]. The measurement set-up is shown in Fig. 6.

High density polyethylene lenses with a focal length of 120 mm are used to collimate and focus the beam. In the transmission experiment, a sample and a reference pulse are measured with and without sample in the propagation path. A window function is applied to the time-domain data to remove unwanted multiple reflections [14]. The frequency dependent index of refraction $n(f)$ and the absorption coefficients $\alpha(f)$ of the samples are calculated from the phase and amplitude information of the Fourier spectra of the pulses in the frequency range between 0.1 and 1 THz [15]. These measurements are performed on samples with smooth surfaces to avoid scattering losses which would result in incorrect material parameters. In case of the ingrain wallpaper a 1.14 mm thick, mechanically pressed stack of single sheets served as sample.

The obtained refractive indexes and absorption coefficients are displayed in Fig. 7.

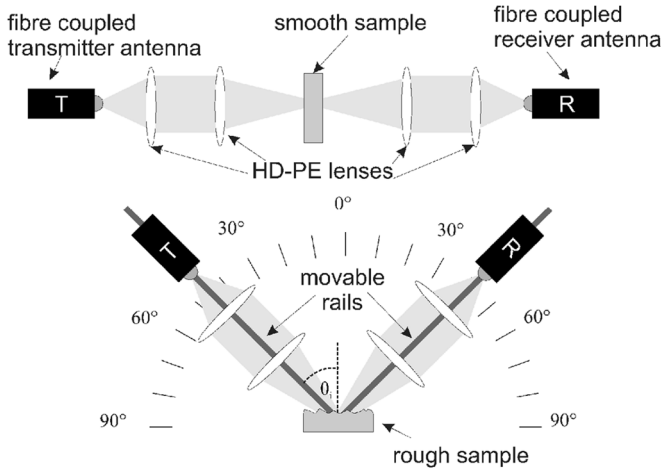

Fig. 6. THz measurement setup in transmission (top) and reflection geometry (bottom). Index of refraction and absorption coefficient, which are measured in the transmission setup, are used to model the results of the reflection measurements.

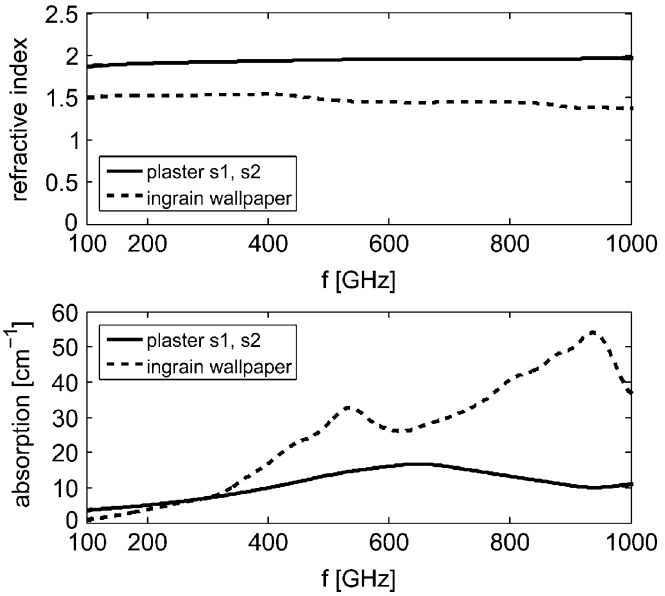

Fig. 7. Measurements of refractive index (top) and absorption coefficient (bottom) of the investigated samples in transmission geometry.

In reflection geometry the transmitter, receiver and lenses are mounted on a movable rail allowing the measurements to be performed for six different angles, i.e., 25°, 30°, 40°, 50°, 60° and 70° for both TE and TM polarization. A sample and a reference measurement where a blank copper plate replaces the sample are performed. The ratio of the Fourier spectra yields the frequency dependent reflection coefficients.

B. Reflection Coefficient Simulations

Furthermore, we calculate the reflection coefficients $\mathrm{r_{TE}}$ and $\mathrm{r_{TM}}$ from our measurements of absorption coefficients and refractive indexes using the conventional Fresnel equations, as in [7]. These coefficients are then multiplied by the Rayleigh factors ρ of the corresponding materials taking into account the different standard deviations of the surface height in order to get $\mathrm{r'_{TE}}$ and $\mathrm{r'_{TM}}$.

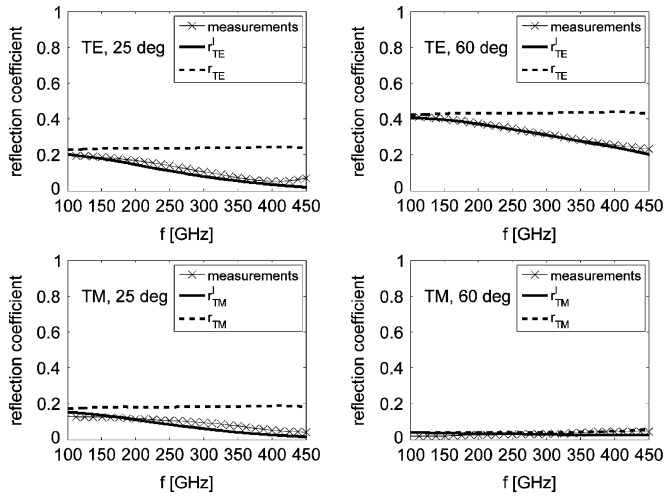

Fig. 8. Calculated magnitude of reflection coefficients $\mathrm{r_{TE}}$ and $\mathrm{r_{TM}}$ and of modified reflection coefficients $\mathrm{r'_{TE}}$ and $\mathrm{r'_{TM}}$ and direct reflection measurements of ingrain wallpaper in the frequency range from 100 to 450 GHz for two angles of incidence of TE and TM polarized waves: 25°, 60°

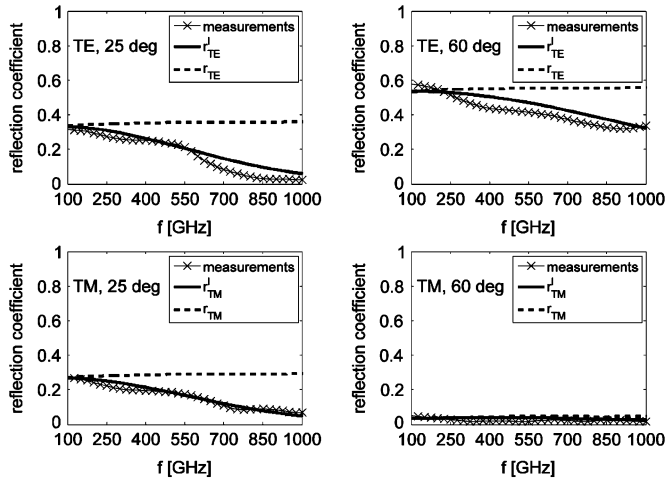

Fig. 9. Calculated magnitude of reflection coefficients $\mathrm{r_{TE}}$ and $\mathrm{r_{TM}}$ and of modified reflection coefficients $\mathrm{r'_{TE}}$ and $\mathrm{r'_{TM}}$ and direct reflection measurements of plaster sample 1 in the frequency range from 100 to 1000 GHz for two angles of incidence of TE and TM polarized waves: 25°, 60°.

The calculated magnitude of reflection coefficients $\mathrm{r_{TE}}$ and $\mathrm{r_{TM}}$ (dashed lines) as well as the calculated magnitude of modified reflection coefficients $\mathrm{r'_{TE}}$ and $\mathrm{r'_{TM}}$ (solid lines) for the ingrain wallpaper are shown for illustration in Fig. 8 for TE and TM polarized waves for the frequency range between 100 and 450 GHz and two different angles of incidence (25° and 60°). The corresponding curves for plaster sample 1 and plaster sample 2 are shown for an extended frequency range between 100 and 1000 GHz in Figs. 9 and 10, respectively, since a smooth absorption curve as shown in Fig. 7 allowed for a more reliable modeling at higher frequencies in this case. The directly measured reflection coefficients (interconnected symbols) are shown for comparison. Additionally, in Fig. 11 the calculated magnitude of modified reflection coefficients $\mathrm{r'_{TE}}$ and $\mathrm{r'_{TM}}$ as well as the directly measured values for wallpaper and plaster sample 2 are shown as a function of angle of incidence for TE and TM polarized waves at the frequency of 350 GHz.

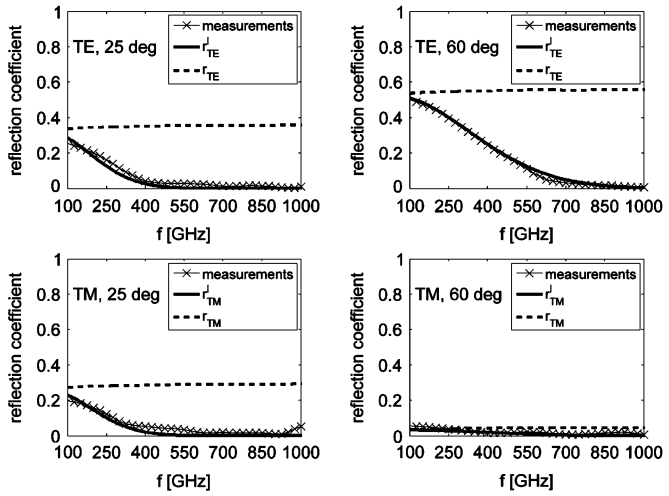

Fig. 10. Calculated magnitude of reflection coefficients $\mathrm{r_{TE}}$ and $\mathrm{r_{TM}}$ and of modified reflection coefficients $\mathrm{r'_{TE}}$ and $\mathrm{r'_{TM}}$ and direct reflection measurements of plaster sample 2 in the frequency range from 100 to 1000 GHz for two angles of incidence of TE and TM polarized waves: 25°, 60°.

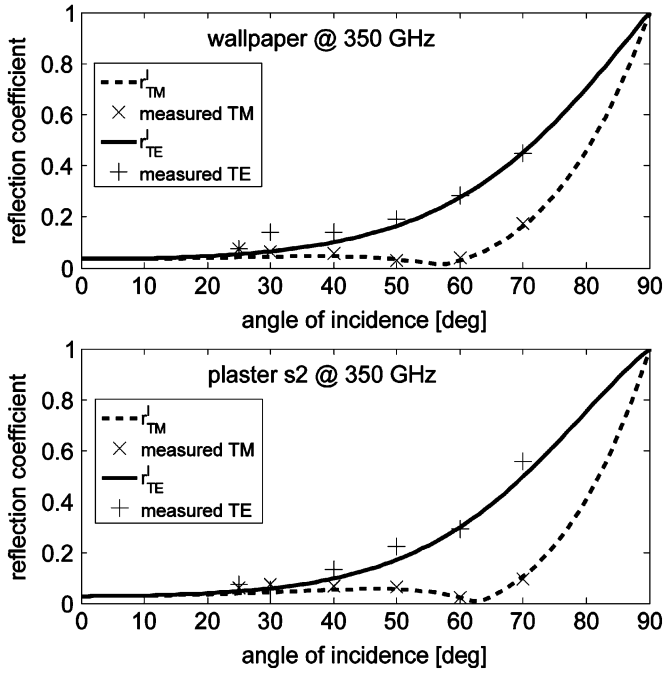

Fig. 11. Calculated magnitude of modified reflection coefficients $\mathrm{r'_{TE}}$ and $\mathrm{r'_{TM}}$ and direct reflection measurements of wallpaper and plaster sample 2 for angles of incidence between 0° and 90° at a frequency of 350 GHz for TE and TM polarized waves.

A good agreement between the simulated modified reflection coefficients $\mathrm{r'_{TE}}$ and $\mathrm{r'_{TM}}$ and the measured reflection coefficients can be found for all materials, incident angles, polarization types and frequencies. The simulated conventional reflection coefficients $\mathrm{r_{TE}}$ and $\mathrm{r_{TM}}$ conform with the measured data only for long wavelengths, depending on the material roughness, angle of incidence and polarization. Except for these limited cases the simulated conventional reflection coefficients deviate significantly from the measured ones. The difference becomes more and more significant as the frequency increases and is correlated to the parameter g.

For frequencies and angles of incidence for which the parameter g takes on values greater than 1, the specular reflections are strongly diminished. Also, for a given angle of incidence and polarization the amplitude of the reflection coefficients decreases with increasing frequency. This is expected, since with an increase in frequency, the effective roughness of the material (described by the parameter g) grows along with the scattering losses in the specular direction.

C. Ray-Tracing Signal Coverage Simulations

A simple illustration of the application of the modified scheme for the calculation of reflection coefficients to channel modeling at THz frequencies is shown by an example of ray-tracing simulated signal coverage at 350 GHz in an indoor scenario with and without rough materials. Link budget analysis for indoor application scenarios shows that future THz communication systems will have to work with high gain antennas, directed for maximum gain to compensate for high free-space losses [3], [4]. Around 32 dB gain for each single antenna will be needed to support 10 m links. In order for such systems to be robust they would have to operate with different directed NLOS paths (reflections from walls etc.) to avoid shadowing by moving objects (e.g., people). Any viable communication would then take place with antennas looking at each other either directly (LOS case) or indirectly through reflections in the specular direction (concept of directed NLOS paths, [3]). Different specular paths could be potentially realized either with a multi-antenna or a phased-array antenna system. The function of such an antenna system would be to find optimum paths at any given time.

The requirement that future THz communication systems will have to rely on high gain antennas has a direct impact on the propagation paths that have to be considered in propagation modeling. In [16] it is shown with ray-tracing simulations and verified with measurements that when working with directive antennas in indoor environments multipath sources can be neglected as they do not contribute significantly to the power delay profile and hence are irrelevant for a communication system. Any multipath coming from outside of the maximum gain direction of the antenna will be attenuated by the antenna radiation pattern. In [16] it is shown that the 3 dB beamwidth should be smaller than 15° to suppress multipath effectively. Antennas that we take into account are high gain (32 dB) and consequently they have small 3 dB beamwidths (e.g., 5° when realized as conical horns). Hence, they will attenuate efficiently any multipath that will come from outside of their maximum gain direction. In our case the incoherent diffuse scattering is considered as multipath and is therefore neglected. Moreover, calculations of the scattered power at 350 GHz show that the specular term dominates over the diffuse incoherent scattering for both considered cases of rough plaster surfaces (at least 15 dB offset between incoherent parts and specular terms).

We simulate single non-line-of-sight (NLOS) specular paths of propagation in a room where there are only walls, i.e., without windows, furniture or any other objects. The dimensions of the room are 6 m × 5 m × 2.5 m. The transmitter with an output power of 0 dBm is positioned in the middle of the room just below the ceiling at the point x = 3 m, y = 2.5 m, z = 2.4 m,

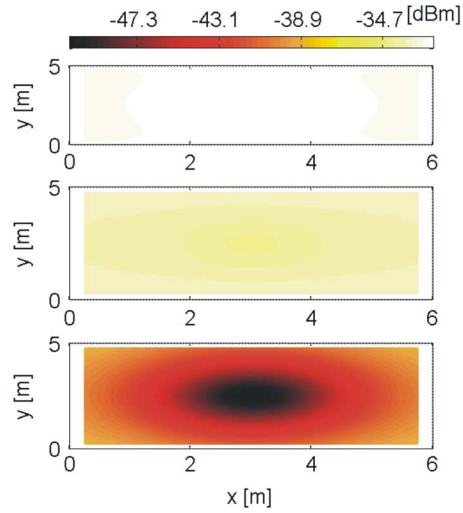

Fig. 12. Ray-tracing simulation of the received power of single reflected TE polarized plane waves in a room with (top to bottom): smooth plaster walls, slightly rough plaster walls (plaster sample 1) and rough plaster walls (plaster sample 2).

with the origin located in the bottom left corner. The position of the receiver is varied in the plane 1 m above the floor. It is assumed that both transmitter and receiver are equipped with antenna systems in order to gather transmitted power of different possible single NLOS paths. For each single path antennas have 32 dB gain and are directed for maximum radiation. The coverage simulations are performed for a frequency of 350 GHz for three cases:

1) the walls are covered only with smooth plaster;
2) the walls are covered only with plaster with a small roughness (plaster sample 1);
3) the walls are covered only with plaster with a considerable roughness (plaster sample 2).

The plane of the receiver at z = 1 m is sampled with 15 points in the x direction and 13 points in the y direction keeping a distance offset of 0.25 m from the walls. At each of the total 195 receiver positions the power in the single reflected paths is summed up including the free-space propagation and the reflection losses. The results of the simulations for TE polarized plane waves are shown in Fig. 12.

The total received power at each receiver position is dominated by the reflections from the ceiling, as in this case the distance from the transmitter to the respective receiver is the shortest of all possible paths. Varying between -30.8 and -31.3 dBm, the received power in the room with smooth plaster walls decreases only very slightly from the middle of the room towards the walls. The distance that the single path signals reflected from the ceiling must travel increases when the receiver moves away from the transmitter towards the walls. However, the increasing free-space path losses are almost completely compensated for by decreasing reflection losses, as the angle of incidence increases. In the case of a room with slightly rough walls the received power is between -32.1 and -33.2 dBm. As previously, the power does not vary considerably throughout the room. Yet, in this case the power distribution is inverted, i.e., the power increases towards the walls. This is due to the property of roughness that causes the

material reflectivity for smaller angles of incidence to be far more affected than for larger angles. The reflected power is reduced compared to the power predicted by the conventional Fresnel equations. For the room with rough walls the received power varies between -38.2 and -51.6 dBm maintaining the inverted character. Here, the influence of roughness is clearly visible. The reflectivity at smaller angles, that corresponds to positions of the receiver near the middle of the room is diminished heavily, while it increases rapidly for larger angles. This decrease in the reflectivity losses dominates over the increase in the free-space propagation losses. Hence, in the case of significant roughness, the received single reflected power increases considerably when the receiver moves away from the transmitter towards the walls. This phenomenon depends on the distribution of angles of incidence and therefore on the placement of the transmitter and the choice of the receiver positions in potential indoor THz cells.

Also, the absolute power levels are strongly influenced by diffuse scattering. If the roughness is not taken into account properly in the propagation modeling the received power levels will be miscalculated by 1.5 dB for the scenario with plaster sample 1 and 12.2 dB for the scenario with plaster sample 2 on average when compared to the power levels predicted for a scenario with smooth materials only. Similar calculations performed for TM polarized waves yield an average error of 1.8 dB and 14.7 dB, respectively. This clearly shows the importance of including scattering effects in specular direction in propagation modeling for future indoor THz communication systems with high gain antennas.

IV. Conclusion

We extended the approach from [7] for the modeling of the reflectivity of optically thick, smooth building materials at THz frequencies to materials with a rough surface. The extension is based on multiplying the conventional Fresnel equations with a Rayleigh factor obtained from the knowledge of surface roughness statistics by Kirchhoff theory of scattering. Reliably calculated reflection losses in specular direction are required for an accurate prediction of the signal propagation in NLOS scenarios of future indoor THz communication systems with high gain antennas. The theory is in good agreement with direct measurements of the reflection properties of typical rough building materials.

Acknowledgment

The authors thank Dr. M. Neugebauer from the Physikalisch-Technische Bundesanstalt in Braunschweig, Germany for performing the surface roughness measurements.

References

[1] T. Nagatsuma, "Exploring sub-terahertz waves for future wireless communications," in *IEEE 31st Int. Conf. on IRMMW and 14th Int. Conf. on Terahertz Electronics*, China, Sep. 2006, p. 4.

[2] A. Hirata, T. Kosugi, H. Takahashi, R. Yamaguchi, F. Nakajima, T. Furuta, H. Ito, H. Sugahara, Y. Sato, and T. Nagatsuma, "120-GHz-band millimeter-wave photonic wireless link for 10-Gb/s data transmission," *IEEE Trans. Microw. Theory Tech.*, vol. 54, no. 5, pp. 1937–1944, 2006.

[3] S. Cherry, "Edholm's law of bandwidth," *IEEE Spectrum*, vol. 41, pp. 19–50, 2004.

[4] R. Piesiewicz, T. Kleine-Ostmann, N. Krumbholz, D. Mittleman, M. Koch, and T. Kürner, "Concept and perspectives of future ultra broadband THz communication systems," in *IEEE 31st Int. Conf. on IRMMW and 14th Int. Conf. on Terahertz Electronics*, China, Sep. 2006, p. 96.

[5] N. Krumbholz, K. Gerlach, F. Rutz, M. Koch, R. Piesiewicz, T. Kürner, and D. Mittleman, "Omnidirectional terahertz mirrors: A key element for future terahertz communication systems," *Appl. Phys. Lett.*, vol. 88, p. 202905, 2006.

[6] N. Hiromoto, R. Fukasawa, and I. Hosako, "Measurement of optical properties of construction materials in the terahertz region," in *IEEE 31st Int. Conf. on IRMMW and 14th Int. Conf. on Terahertz Electronics*, China, Sep. 2006, p. 157.

[7] R. Piesiewicz, T. Kleine-Ostmann, N. Krumbholz, D. Mittleman, M. Koch, and T. Kürner, "Terahertz characterisation of building materials," *IEE Electron. Lett.*, vol. 41, no. 18, pp. 1002–1004, 2005.

[8] L. Tsang, J. A. Kong, K. H. Ding, and C. O. Ao, *Scattering of Electromagnetic Waves: Numerical Simulations*. New York: Wiley, 2001.

[9] K. F. Warnick and W. C. Chew, "Numerical simulation methods for rough surface scattering," *IoP Waves in Random Media*, vol. 11, no. 1, pp. R1–R30, 2001.

[10] P. Beckmann and A. Spizzichino, *The Scattering of Electromagnetic Waves from Rough Surfaces*. Norwood, MA: Artech House, 1987, pp. 80–98.

[11] R. Vaughan and J. B. Andersen, "Channels, propagation and antennas for mobile communications," in *IEE Electromagnetic Waves Series*, London, U.K., 2003, vol. 50, pp. 105–115.

[12] *Alicona Imaging InfiniteFocus, Alicona Imaging GmbH*, [Online]. Available: www.alicona.com

[13] D. Mittleman, "Terahertz Imaging," in *Sensing with Terahertz Radiation*, D. Mittleman, Ed. : Springer, 2003, pp. 117–153.

[14] R. W. Ramirez, *The FFT: Fundamentals and Concepts*. Englewood Cliffs, NJ: Prentice-Hall, 1985.

[15] L. Duvillaret, F. Garet, and J.-L. Coutaz, "A reliable method for extraction of material parameters in Terahertz time-domain spectroscopy," *IEEE J. of Quantum Electron.*, vol. 2, no. 3, pp. 739–746, 1996.

[16] P. F. Driessen, "Gigabit/s indoor wireless systems with directional antennas," *IEEE Trans. Commun.*, vol. 44, no. 8, pp. 1034–1043, 1996.

Radoslaw Piesiewicz (S'04) was born in Koszalin, Poland, in 1976. He received the International Baccalaureate Bilingual Diploma IB, issued in Geneva, Switzerland, from the "III LO im Marynarki Wojennej RP," in 1996. He studied economics at the Warsaw School of Economics, Warsaw, Poland, from 1996 to 1997 and electrical engineering at the Technical University of Gdansk, Poland, from 1997 to 2002, where he received the M.S.E.E. degree (with highest honors) in microwave engineering. He is currently working toward the Ph.D. degree in the Institut für Nachrichtentechnik at the Technical University of Braunschweig, Germany.

From 2002 to 2004, he was with Fraunhofer Institut IZM, Advanced Systems Engineering in Paderborn, Germany, where he worked on electromagnetic compatibility problems in multilayer circuits in the framework of the EU Project MESDIE. Since 2004, he has been a project Research Engineer in the Terahertz Communications Lab in Braunschweig. His research interests include PHY layer aspects of ultrabroadband multigigabit wireless communication systems at frequencies above 60 GHz. The focus is on system modeling, simulation and design as well as on the propagation aspects in bound and unbound media, including measurements and modeling. He is an active expert evaluator in the field of communication systems for the European Commission in Brussels.

Christian Jansen (S'07) is working toward the electrical engineering degree at the Technical University (TU) of Braunschweig, Germany.

Currently, he is stipendiary of the Chair of the TU Braunschweig. In 2006, he performed research in the field of terahertz technology at Rice University, Houston, TX, on a DAAD scholarship.

Mr. Jansen received a scholarship from the German Academic Exchange Service (Deutscher Akademischer Austauschdients or DAAD).

Daniel Mittleman received the B.S. degree in physics from the Massachusetts Institute of Technology, Cambridge, in 1988 and the M.S. and Ph.D. degrees both in physics, from the University of California, Berkeley, in 1990 and 1994, respectively.

He 1988, he joined the research group of Dr. Charles Shank at the University of California, Berkeley. His primary research involved the spectroscopy of semiconductor nanocrystals using laser pulses with durations of less than 20 femtoseconds, at wavelengths from 480 to 670 nm. These experiments were performed in collaboration with the Alivisatos group in the Chemistry Department at Berkeley and were carried out at the Lawrence Berkeley National Laboratory. He then joined the research group of Dr. Richard Freeman, as a Postdoctoral Member of the Technical Staff at AT&T Bell Laboratories. While there, he pursued research into high harmonic generation in noble gases using a 100 femtosecond, 1 terawatt laser system. When he left Bell Labs in early 1995, he began working with Dr. Martin Nuss, who had recently pioneered the use of THz time-domain spectroscopy for imaging. His work in this laboratory included the non-contact characterization of doped semiconductor wafers using the THz Hall effect, the construction of a THz imaging system in a reflection geometry for use in "T-Ray Tomography" measurements, and the THz spectroscopy of inverse micelles of water in heptane. During this time, AT&T split into three companies, and most of Bell Labs became part of one of the companies, Lucent Technologies. In September 1996, he joined the ECE Department at Rice University, Houston, TX, where he is affiliated with the Rice Quantum Institute.

Thomas Kleine-Ostmann was born in Lemgo, Germany, in 1975. He received the M.Sc. degree in electrical engineering from Virginia Polytechnic Institute and State University, Blacskburg, in 1999, and the Dipl.-Ing. degree in radio frequency engineering and the Dr.-Ing. degree, both from the Technical University Braunschweig, Germany, in 2001 and 2005, respectively.

He worked as a Research Assistant in the Ultrafast Optics Group at the Joint Institute of the National Institute of Standards and Technology and the University of Colorado, Boulder (JILA) and in the Semiconductor Group at Physikalisch-Technische Bundesanstalt, in Braunschweig, Germany, before he started working on his Ph.D. in the field of THz spectroscopy. Since 2006, he has been working as a permanent Scientist in the Electromagnetic Fields Group at Physikalisch-Technische Bundesanstalt. Currently, he is working on realization and transfer of the electromagnetic field strength, electromagnetic compatibility and THz metrology.

Dr. Kleine-Ostmann is a member of the German Association of Electrical Engineers (VDE). He received the Kaiser-Friedrich Research Award in 2003 for his work on a continuous-wave THz imaging system.

Martin Koch was born in Marburg, Germany, in 1963. He received the Diploma and Ph.D. degree in physics from the University of Marburg, in 1991 and 1995, respectively.

From 1995 to 1996, he was a Postdoctoral Researcher at Bell Labs/Lucent Technologies, Holmdel, NJ. From 1996 to 1998, worked in the Photonics and Optoelectronics Group at the University of Munich. Since 1998, he has been an Associate Professor at the Technical University of Braunschweig, Germany, in the Electrical Engineering Department. In 2003, he did a three month sabbatical at the University of California in Santa Barbara.

Dr. Koch was awarded the Kaiser-Friedrich Research Price Award in 2003.

Thomas Kürner (SM'01) was born in Tailfingen, Germany, in 1964. He received the Dipl.-Ing. degree in electrical engineering and the Dr.-Ing. degree from the University of Karlsruhe, Germany, in 1990 and 1993, respectively.

From 1990 to 1994, he was with the Institut für Höchstfrequenztechnik und Elektronik (IHE) at the University of Karlsruhe, working on wave propagation modelling, radio channel characterization and radio network planning. Until 1994, he was also a Lecturer for the Carl Cranz Series for scientific education, teaching wave propagation modelling, and channel characterization. From 1994 to 2003, he was with the Radio Network Planning Department at the headquarters of the GSM 1800 and UMTS operator E-Plus Mobilfunk GmbH & Co. KG, Düsseldorf, where he was Team Manager of radio network planning support, responsible for radio network planning tools, propagation models, algorithms, processes and parameters. Since 2003, he has been a Professor for Mobile Radio Systems at the Institut für Nachrichtentechnik at the Technical University of Braunschweig, Germany. His research interests are propagation, traffic and mobility models for automatic planning of mobile radio networks, planning of hybrid networks, car-to-X-communication as well as indoor channel characterization for high-speed short-range systems including future terahertz communication systems. He has been engaged in several international bodies like ITU-R SG 3 (radio wave propagation), UMTS Forum Spectrum Aspects Group, COST 231, COST 273, COST 2100, and COST 259, where he chaired the working group "Network Aspects." He was also a Work Package Leader in the European IST-MOMENTUM project working on methods for "Automatic Planning of large-scale Radio Networks."

Dr. Kürner received the "ITG-Förderpreis" Award from the German VDE for his Ph.D. thesis in 1994, and in 1995 he was awarded the IEE/ICAP'93 Best Propagation Paper Award. He was the Vice-Chair of the European Conference on Antennas and Propagation in 2007.